JET-R(96)03

Analysis of a Global Energy Confinement Database for JET Ohmic Plasmas

G Bracco[1], K Thomsen.

JET Joint Undertaking, Abingdon, Oxfordshire, OX14 3EA, UK.
[1] Associazione EURATOM–ENEA sulla Fusione, Centro Ricerche Energia Frascati, C.P.65 – 00044 Frascati, Rome, Italy.

Preprint of a paper to be submitted for publication in Nuclear Fusion

March 1996

ABSTRACT

A database containing global energy confinement data for JET ohmic plasmas from the campaigns 1984-92 has been established. This paper presents an analysis of this database and compares the results with data from other tokamaks such as ASDEX, FTU and TORE SUPRA. The trends of JET ohmic confinement appear to be similar to that observed on other tokamaks.

I. INTRODUCTION

The energy confinement of ohmically heated plasmas is characterized by a linear increase of the confinement time τ_E with density (LOC linear ohmic confinement) followed by a saturation at high density (SOC saturated ohmic confinement) [1]. The value of density at which the saturation takes place, n_{sat}, decreases with machine size. The origin of the two regimes and the respective scalings of τ_E and n_{sat} with the plasma parameters are still under investigation. The behaviour of energy confinement in JET ohmic plasmas has previously been described in a paper [2] which refers to results obtained in the 1984-85 experimental campaigns. The data then had a limited range in line averaged density ($\bar{n} > 1\times10^{19}$ m^{-3}) and the LOC regime was not clearly identified. A subsequent paper [3] addressed the isotope scaling of τ_E in the ohmic regime, by comparing Hydrogen and Deuterium plasmas. A weak mass dependence was observed, lower than the usual $\tau_E \propto M^{0.5}$ reported by other tokamaks [1].

The present work attempts to assess the behaviour of the global energy confinement in JET ohmic plasmas, by examining the data collected in the experimental campaigns from 1984 to 1992, ie. before the installation of the JET pumped divertor. As far as possible, data referring to stationary plasma conditions have been selected for standard JET operating scenarios. The resulting database is also ready to be combined with data from other tokamaks for a study of the size dependence of τ_E in ohmic plasmas.

II. CONFINEMENT DATA DISCUSSION

As usual the energy confinement time is defined as $\tau_E = W/(P_{oh}-dW/dt)$, where W is the plasma energy content and P_{oh} is the total ohmic power. The data have been chosen from the ohmic subset of the JET Transport Database, where the typical time averaging window is 0.2 s for all the quantities involved in the global energy confinement evaluation. For ohmic plasmas, the best estimate of W is the one based on the kinetic data as the precision of W determined by diamagnetism and by equilibrium analysis is of the order of 1 MJ, which is comparable with the typical energy content for ohmic plasmas. The electron energy content is determined from the measurements of electron temperature T_e and density n_e, while the ion energy content is estimated from the neutron yield measurement for Deuterium plasmas. Electron temperature is

measured in JET both by ECE (Electron Cyclotron Emission) diagnostics and by a LIDAR Thomson scattering system. ECE data are available for the full 1984-92 database, while LIDAR data are only available from 1988 onwards. The absolute calibration of ECE provides peak electron temperatures 13 % lower than LIDAR data, and it has been checked that this small discrepancy does not depend on the different operation periods, nor on the plasma parameters (B_t, T_e or n_e). Here it has been decided to rely on T_e as measured by ECE for the entire 1984-92 period, taking into account the discrepancy between LIDAR and ECE as an estimate of the systematic error on the measurement. Line averaged values of the electron density are measured by a DCN interferometer system and the n_e profile is obtained using an approximate reconstruction of the plasma geometry [4]. To estimate the ion energy content from neutron yield for Deuterium plasmas, requires an assumption on the Deuterium concentration $C_D = n_D/n_e$. The standard data processing for 1984-92 has assumed $C_D = 0.5$, which was typical of the very first years of operation [2]. From 1988 onwards the vessel conditioning with He GDC (glow discharge cleaning) and from 1989 onwards also the operation with Beryllium have reduced Z_{eff}, near to 1 in many operating conditions, so that this assumption is somewhat pessimistic. However, it must be pointed out that in the temperature range 1-3 keV, typical for the ion temperature T_i in ohmic plasmas, the neutron yield Φ_{DD} scales as $\Phi_{DD} \approx C_D^2\ T_i^{4.4}$ so that, for a fixed Φ_{DD} value the ion energy content W_i scales as $W_i \approx C_D^{0.54}$. As a result, the $C_D = 0.5$ assumption would underestimate W_i and W at most by 40% and 20%, respectively. The overall systematic error on W is of this order of magnitude. In the following sections the results obtained using the alternative approach of estimating C_D from Z_{eff}, and making an assumption on the dominant plasma impurity, will be also discussed. For a good evalution of the ohmic power, it has been noticed that the time average window of 0.2 s is not sufficient, as both P_{oh} and the voltage at the plasma surface V_{sur} show large oscillations, with a typical frequency of a few Hertz. For this reason it has been decided to re-compute the values of V_{sur} and P_{oh}, performing an average over a 1 s time window for the full 1984-92 database.

III. DATA SELECTION CRITERIA

The ohmic subset of the Transport Database 1984-92 consists of more than 20000 observations, with each discharge typically accounting for 3 observations (data from 3 different times). A set of selection criteria has been applied to reduce this large amount of data, attempting to restrict the database to stationary plasma conditions and in standard situations for which all the relevant data from the diagnostics systems are available. In Table 1 the main rejection criteria are summarized together with the number of rejected observations for each criterion. The criteria are discussed in the following.

Table 1. *Number of observations rejected from the ohmic subset of the JET transport database by the various selection criteria.*

Selection criteria	**number of rejected observations**
Reference time points for auxiliary heating	4000
V_{sur} and V_{axis} differing more than 25%	3800
T_e^{ax} and T_e^{max} differing more than.10%	1100
Time points at less than .7 s between each others	900
Relative error on $n_e(r)$ greater than 20%	800
Main ion mass unknown	500
No horizontal bremsstrahlung after 1985	500
Plasma current not in flat top phase	450
No neutron data for Deuterium plasmas	300
B_t lower than 1.6 T	200
Strong density ramps	100
Other reasons	400

Ohmic reference points for auxiliary heated phases have been discarded. These data are taken typically 0.2 s before the onset of auxiliary heating so that the averaging procedure for V_{sur} and P_{oh} can not be applied. For the same reason, only one of the observations for times differing less than 0.7 s in the same plasma discharge has been kept. An approximate model [4] has been used to evaluate the loop voltage on the plasma magnetic axis V_{axis} and an example [2] of the time behaviour of V_{sur} and V_{axis} is shown in figure 1. Hence data taken at the beginning of the current flat top or in non stationary plasma current situations can be, and have been, excluded by imposing limits on the ratio between V_{axis} and V_{sur}, ie. $0.75<V_{axis}/V_{sur}<1.25$. In figure 2 examples of electron temperature profiles are shown, to illustrate the characteristics of the data rejected when the electron temperature on axis T_{e0} and the maximum electron temperature T_e^{max} differ in a significant way. As it is attempted here to select discharges in the standard ohmic regime, possibly with sawtooth activity, the cases of hollow T_e profiles, probably indicating an important role of radiation at the plasma centre, have been rejected. The data rejected by this criterion are mainly from the years before 1988. The data with $B_t < 1.6$ T have been discarded because of unreliable measurements of T_e by the ECE diagnostics at low magnetic fields. The subset of data reported rejected for other reasons in Table 1 includes data discarded for bad density measurements or for being in the slide away regime with non thermal ECE emission. The selection procedure results in a subset with 7000 observations, which is the ohmic database discussed in the following sections.

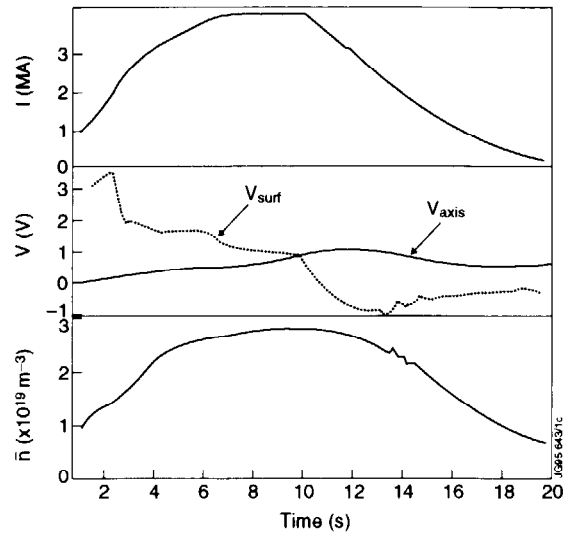

Figure 1. Plasma current, loop voltage at the plasma surface and on the magnetic axis, line averaged density for discharge 4591, reproduced from [2].

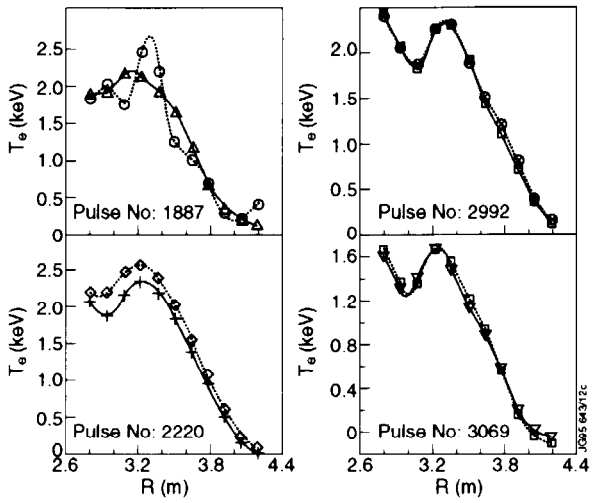

Figure 2. Examples of electron temperature radial profiles for data rejected from the JET Transport Database if T_{e0} and T_e^{max} differ by more than 10%.

As shown in Table 2, most of the data in this database are from limiter discharges with Deuterium plasma. An examination of the Deuterium subset reveals the following. Figure 3.a shows that most of the limiter discharges have an elongation κ in the range 1.3-1.5, while for x-point discharges κ=1.7-1.9. Only very few circular plasma discharges are available. These have a reduced minor radius a and were produced for the study of the major radius dependence of confinement, reported in [2]. The minor radius, figure 3.b, is typically in the range a=1.13-1.22 m for limiter discharges, while the x-point configurations usually have a smaller value of a. The values of the cylindrical safety factor q_{cyl} (defined as $q_{cyl}=5a^2\kappa B_t/RI_p$) are concentrated in the lower q_{cyl} range, as shown in figure 3.c.

Table 2. *Number of data retained in the database for each ion species and plasma configuration:*

Ion species	**LIMITER**	**X-point**
Deuterium	4369	1296
Hydrogen	196	78
Helium 3	316	39
Helium 4	657	214

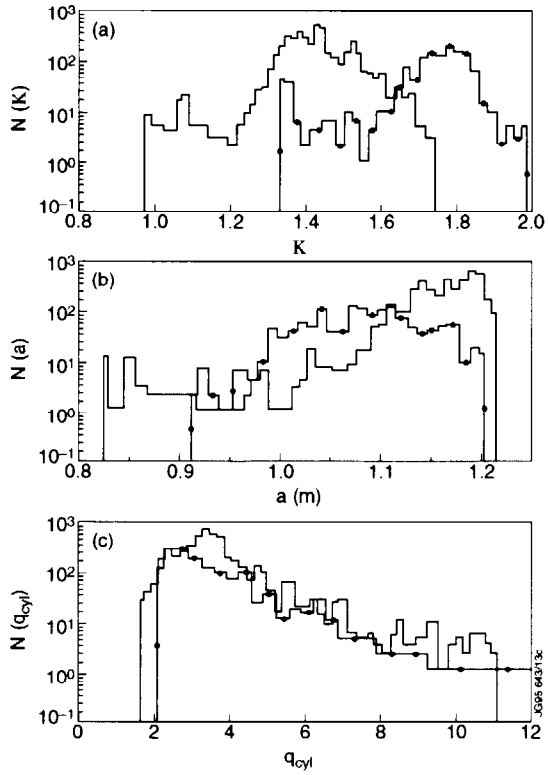

Figure 3. Distributions of the number of data available in the database as a function of a) the elongation κ; b) the minor radius a; and c) q_{cyl} for Deuterium plasmas both in limiter (continuous line) and divertor configuration (line and dot).

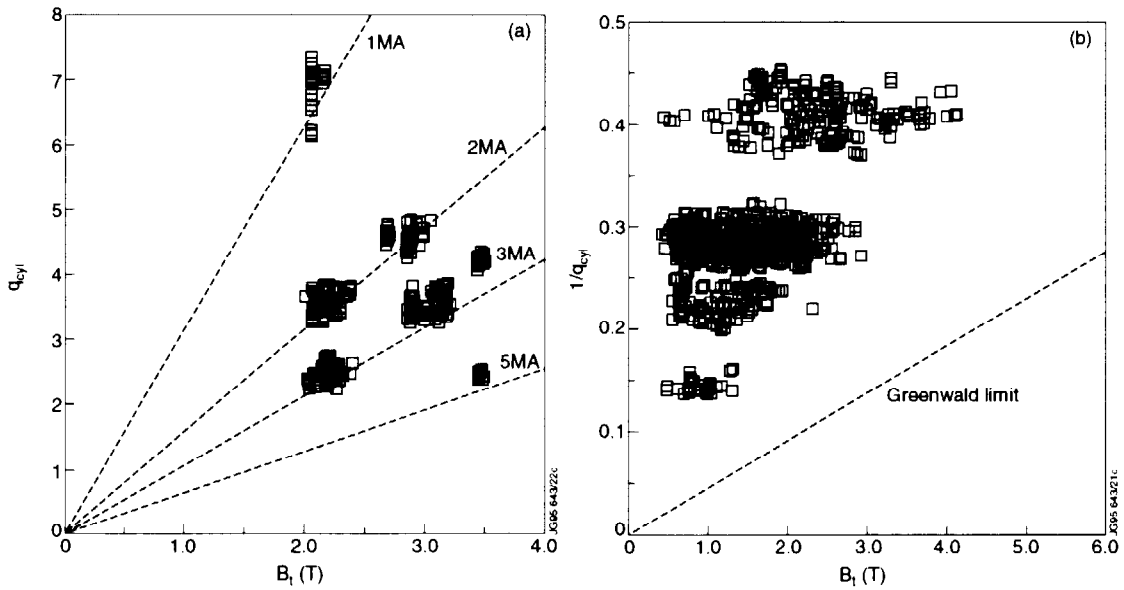

Figure 4. Data for Deuterium plasmas in limiter configuration: a) q_{cyl} versus B_t; b) Hugill diagram, in which the dotted line indicates the Greenwald limit.

A further restricted Deuterium subset has been established by selecting only discharges with limiter configuration, κ = 1.3-1.5, a = 1.13-1.22 m and 4 ranges of q_{cyl}, q_{cyl}=2.2-2.8, 3.2-3.8, 4-5 and 6-8. This results in a subset of about 1400 observations. To this selection the x-point data in the range κ=1.7-1.9 with a=1.05-1.22 m have been added. In figure 4.a the values of q_{cyl} and B_t are plotted for this Deuterium limiter subset, which can be used to study the confinement behaviour. The plasma current is in the range 1-5 MA. From the Hugill diagram, figure 4.b, it can be concluded that the highest density for Deuterium plasmas is well below the Greenwald limit. Helium plasmas, which will be shown later, reach higher density values. In figure 5, the ratio between the central electron temperature T_{e0} and the volume average $<T_e>$ is shown as a function of q_{cyl}. In the standard ohmic regime the value of $T_{e0}/<T_e>$ should satisfy the constraint $q_{cyl}^{2/3} < T_{e0}/<T_e> < q_{cyl}$ [5], which is indeed the case for the JET data. In FTU [6] a set of discharges for which the presence of sawtooth activity has been confirmed, shows that the constraint is satisfied even in the stronger form $T_{e0}^{3/2}/<T_e^{3/2}>=q_{cyl}$. It can be concluded that the T_e peaking factor of the selected JET data indicates that the data refer to a standard ohmic regime.

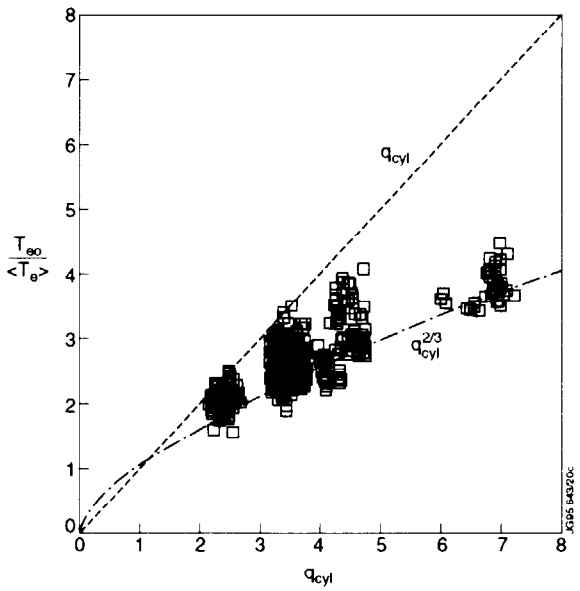

Figure 5. Electron temperature peaking factor $T_{e0}/<T_e>$ versus q_{cyl} for Deuterium plasmas in limiter configuration. The dotted lines indicates the limits found by [5].

IV. CONFINEMENT DEPENDENCE ON <n>, B_t, I_p

In figure 6.a, the values of τ_E for q_{cyl}=3.5 and B_t=3T are shown versus density: the LOC regime is clearly identified and a $n_{sat}=1.5\times10^{19}$ m^{-3} can be deduced. In figure 6.b, the value of τ_E is evaluated from the neutron yield by estimating the Deuterium concentration using the Z_{eff} from bremsstrahlung and assuming Carbon is the main impurity. A slight difference in the

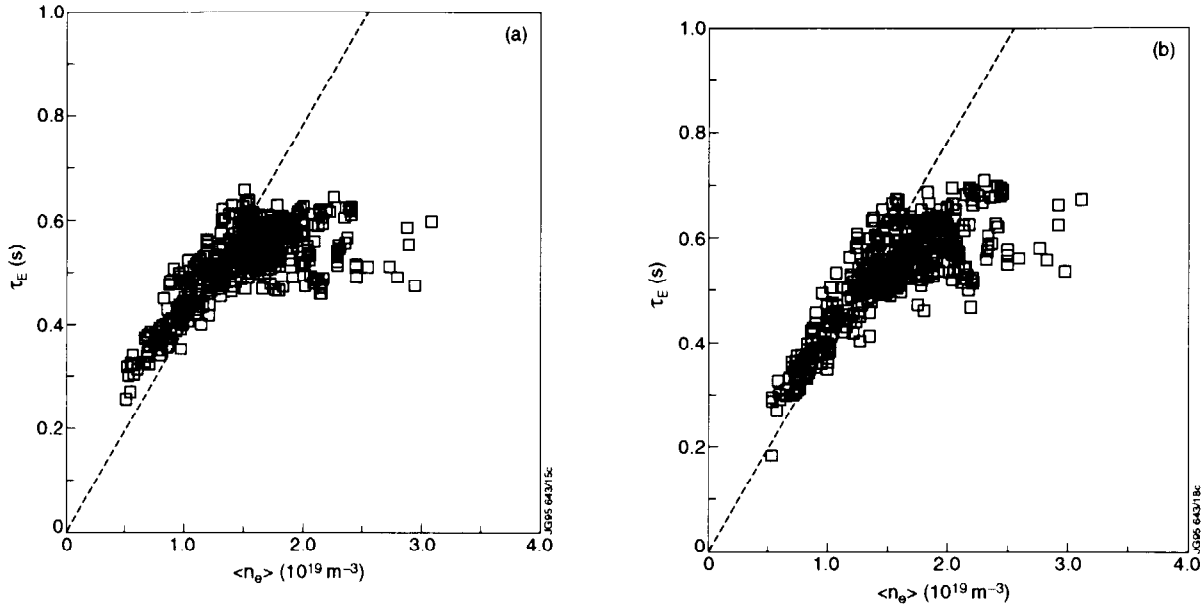

Figure 6. Global energy confinement time versus volume averaged density for Deuterium, limiter I_p=3 MA, B_t=3 T, q_{cyl}=(3-4); the ion energy content has been estimated a) assuming n_D/n_e=0.5; b) assuming Carbon to be the main impurity and Z_{eff} from visible bremsstrahlung; the dotted line provides just a visual reference for comparing the LOC results.

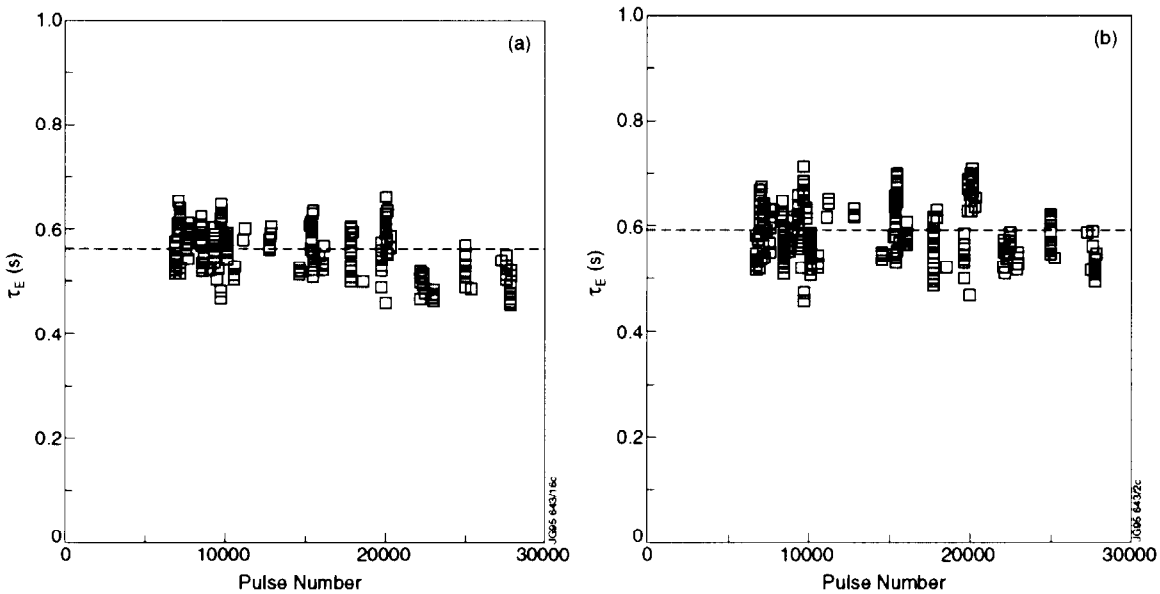

Figure 7. Global energy confinement time in SOC regime versus pulse number for Deuterium, limiter I_p=3 MA, B_t=3 T, q_{cyl}=(3-4), a) and b) as in figure 6.a,b.

LOC regime can be observed. In the SOC regime the values in figure 6.b are somewhat higher. In figures 7.a,b, the values of in the SOC regime (<n> > 1.5×10^{19} m^{-3}) are shown versus the pulse number. The saturated τ_E value is approximately constant during the various experimental campaigns from 1986 to 1992. The averages of the τ_E values shown in figures 7.a,b, resulting from the two ways of evaluating the ion energy content, give τ_E = 0.55 s and

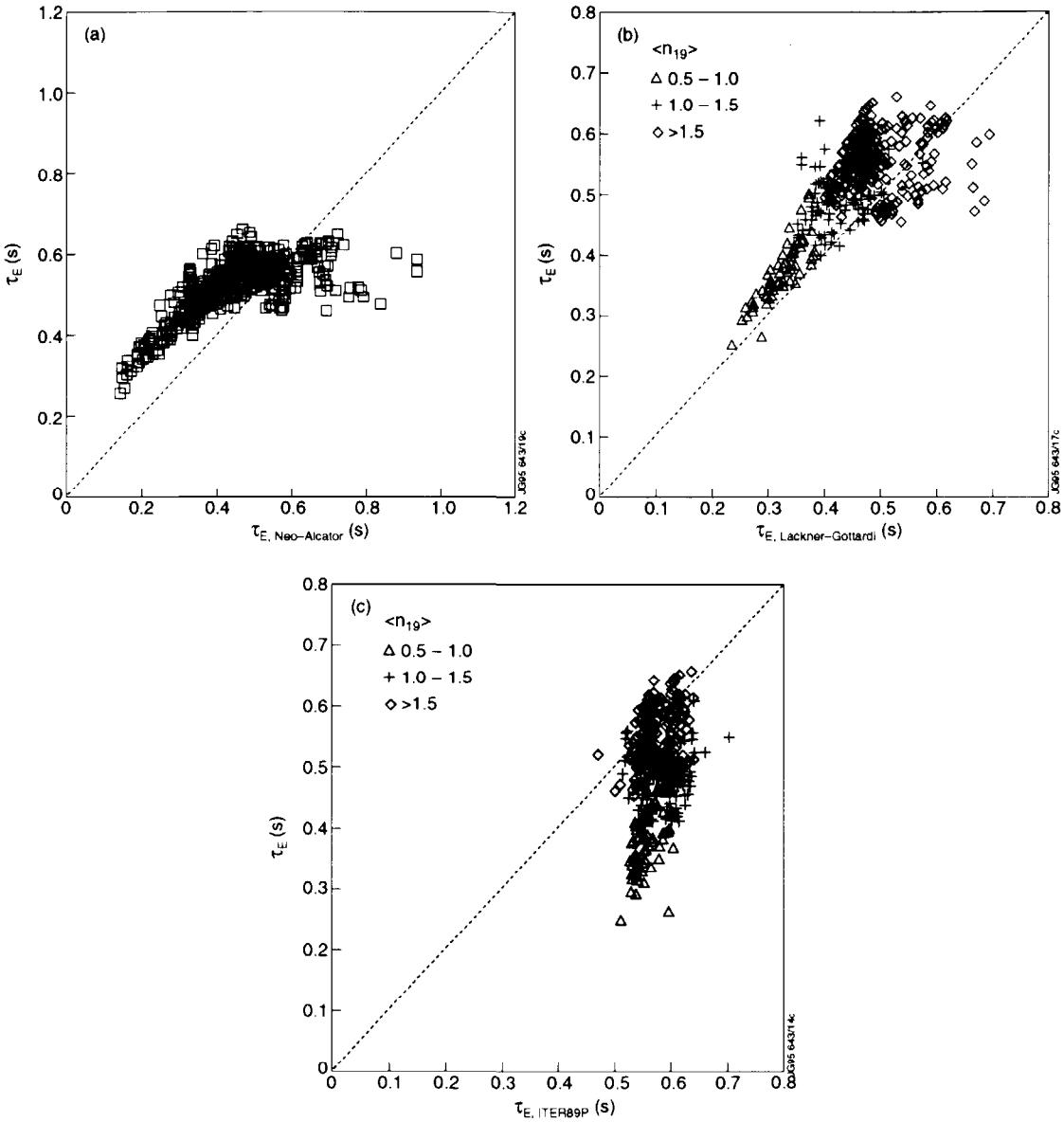

Figure 8. Global energy confinement time versus scalings laws: a) Neo-Alcator; b) Lackner-Gottardi; and c) ITER89P; in b) and c) the diamonds indicates the data in the SOC regime.

$\tau_E = 0.59$ s, respectively. In figure 8, τ_E values are compared with: a) the Neo-Alcator scaling [7], to which a factor $\kappa^{1/2}$ has been added to account for the JET elongation; b) the Lackner-Gottardi scaling [8]; and c) with ITER89P scaling [9]. In the LOC regime the JET data are well above the Neo-Alcator scaling, as observed also on other elongated tokamaks, such as C-MOD [10]. Similarly to what is observed on FTU [11], the Lackner-Gottardi scaling is in rather good agreement with data in the LOC but not in the SOC regime, while ITER89P, on the other hand, seems to agree with the SOC data.

In figures 9 and 10, the energy confinement time is shown versus density for various subselections of the Deuterium limiter dataset, in an attempt to visualise the dependence on B_t,

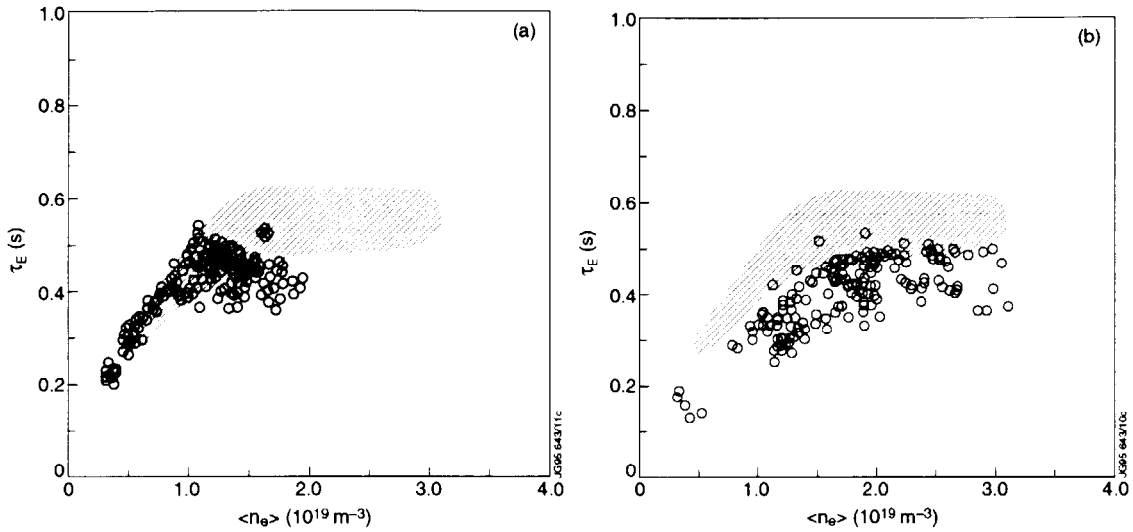

Figure 9. Global energy confinement time versus volume averaged density for a) I_p=2MA, B_t=2.2T, q_{cyl}=(3-4); and b) I_p=3 MA, B_t=2.2T, q_{cyl}=(2-3); in both cases the shaded area indicates the results at I_p = 3 MA, B_t = 3 T, q_{cyl}=(3-4) presented in figure 6.a.

I_p and q_{cyl}. Figure 9.a shows that for fixed q_{cyl}, the confinement in the LOC regime does not depend on B_t. However, n_{sat} apparently increases, resulting in a higher value for τ_E, in the SOC regime with increasing B_t. This is also seen for other values of q_{cyl}, as shown in figure 10.a. For fixed I_p, the confinement improves in both the LOC and SOC regimes, as shown in figure 9.b. Finally, figure 10.b indicates that for fixed B_t, the slope with density in the LOC regime decreases with increasing current, whereas the value of the saturated τ_E is unchanged. The trends deduced from figures 9 and 10 are in qualitative agreement with those observed on other tokamaks [1].

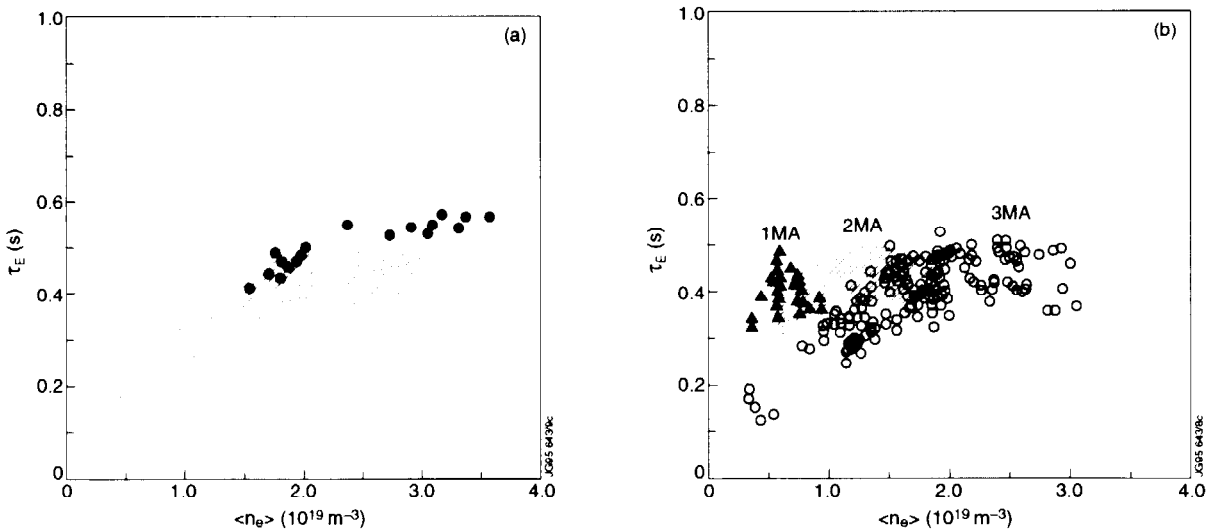

Figure 10. Global energy confinement time versus volume averaged density for a) I_p=5 MA, B_t=3.5 T, q_{cyl}=(2-3), the shaded area indicates the data at B_t=2.2 T at the same q_{cyl} value shown in figure 9.b; and b) B_t=2.2 T, I_p=1, 2 and 3 MA corresponding to q_{cyl}=(2-3), (3-4) and (6-8).

V. SCALINGS FOR W, V_{sur}, $\langle T_e \rangle$ AND τ_E

The Deuterium limiter configuration subset of the database has been used to assess the parameter dependences of the main quantities involved in the global energy confinement analysis, ie. W, $\langle T_e \rangle$, V_{sur} and τ_E. Standard regression techniques have been used to obtain the exponents on I_p, $\langle n \rangle$ and B_t for the scalings (power laws) of W, $\langle T_e \rangle$, V_{sur} and τ_E, shown in table 3. This table also show the corresponding results for ASDEX [12] and FTU [13]. Apart from a stronger B_t dependence on JET, table 3 shows that the dependences on I_p and $\langle n \rangle$ are rather similar in the three tokamaks. For JET the obtained regressions have a good correlation coefficient in the case of W and $\langle T_e \rangle$, while it is worser for τ_E and worst for V_{sur}. This fact was also observed in [12,13]. A better fit for V_{sur} can be obtained, if Z_{eff} is included as a regressor variable. This fit is shown in table 4 for both JET and FTU and it is seen that the scaling trends of V_{sur} on the two tokamaks are similar. Finally in table 5 the correlation matrix between the regression variables is shown.

Table 3. *Exponents of I_p, $\langle n \rangle$ and B_t from the regression of W, $\langle T_e \rangle$, V_{sur} and τ_E for JET, ASDEX [12] and FTU [13]; the errors on the exponents are given in brackets. The R and the RMS error of the fits are also provided.*

W	Tokamak	I_p	$\langle n \rangle$	B_t	R	RMSE %
	JET	0.80(.01)	0.60(.01)	0.36(.01)	0.96	12.5
	ASDEX	0.80(.05)	0.53(.03)	0.13(.05)		
	FTU	0.94(.01)	0.38(.01)	0.16(.04)		
$\langle T_e \rangle$		I_p	$\langle n \rangle$	B_t	R	RMSE %
	JET	1.01(.07)	−.57(.01)	0.22(.06)	0.89	13.1
	ASDEX	0.93(.06)	−.61(.04)	0.04(.07)		
	FTU	1.21(.01)	−.69(.01)	−.04(.04)		
V_{sur}		I_p	$\langle n \rangle$	B_t	R	RMSE %
	JET	0.20(.02)	0.22(.01)	−.38(.02)	0.76	9.8
	ASDEX	0.19(.03)	0.30(.02)	−.31(.03)		
	FTU	0.25(.04)	0.14(.02)	−.28(.11)		
τ_E		I_p	$\langle n \rangle$	B_t	R	RMSE %
	JET	−.40(.01)	0.39(.01)	0.79(.01)	0.84	11.8
	ASDEX	−.39(.06)	0.23(.05)	0.44(.07)		
	FTU	−.31(.04)	0.25(.01)	0.44(.04)		

Table 4. *Exponents of Z_{eff}, $<n>$ and B_t for the regression of V_{sur} for JET and FTU [13]; the errors on the exponents are given in brackets.*

V_{sur}	Tokamak	Z_{eff}	<n>	B_t	R	RMSE %
	JET	0.24(.05)	0.39(.05)	−.41(.02)	0.82	8.5
	FTU	0.31(.02)	0.42(.02)	−.30(.08)		

Table 5. *Correlation matrix for the Deuterium, limiter data.*

	log(<n>)	log(B_t)	log(I_p)	log(Z_{eff})
log(<n>)	1.000			
log(B_t)	0.283	1.000		
log(I_p)	0.522	0.552	1.000	
log(Z_{eff})	-0.500	0.184	0.019	1.000

VI. LIMITER AND X-POINT CONFIGURATIONS

The Deuterium data from limiter and x-point plasma configurations with the same values of I_p, q_{cyl} and B_t are compared in figure 11. The confinement time is slightly higher for x-point discharges with the exception of a group of data from 1990 (solid symbols). However, it was mentioned earlier, eg. see figure 3.a, that it is not possible to separate the effect on confinement of the x-point configuration and elongation with the present dataset. The X-point data have κ=1.7-1.9 and a reduced minor radius, figure 3.b. If the x-point data from 1990 is discarded, the dependence on κ is $\tau_E \propto \kappa^{0.53}$ for the combined limiter and x-point dataset.

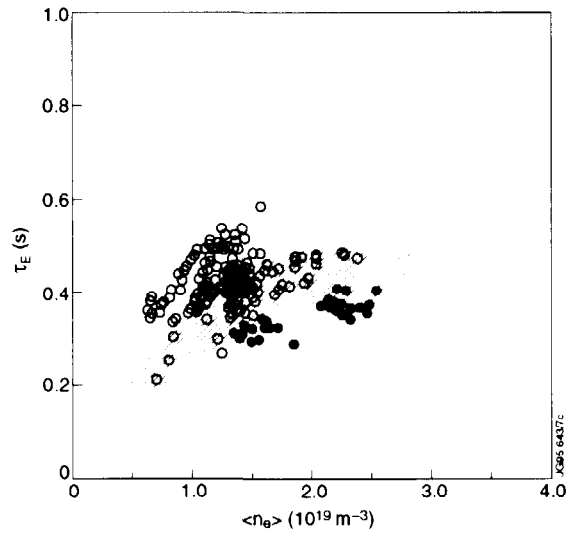

Figure 11. Global energy confinement time versus volume averaged density for I_p=3 MA, B_t=2.2 T, q_{cyl}=(2-3) with x-point configuration, κ=(1.7-1.9); solid symbols correspond to data from 1990; the shaded area indicates the data in the limiter configuration with the same plasma parameters.

VII. ISOTOPE EFFECT

As it can be seen from table 2, the amount of available Hydrogen data is small. Most of these data are from the 1984 campaign, where the quality of the plasma and of the data was poorer than in the later years. As a result, the τ_E values versus density show a large scatter and no firm conclusions can be drawn. The amount of Helium data, He^3 and He^4, available is larger. The operation in He also permits easily access to higher values of density, so that data are available up to the Greenwald limit. The electron energy replacement time, $\tau_E^e = W_e/P_{oh}$, is slightly higher for Helium compared to Deuterium, see figure 12.a (He^3) and 12.b (He^4), but the total energy confinement time is probably similar due to a reduced ion energy content in Helium. A similar energy confinement for Deuterium and Helium plasmas has been observed in many tokamaks [1].

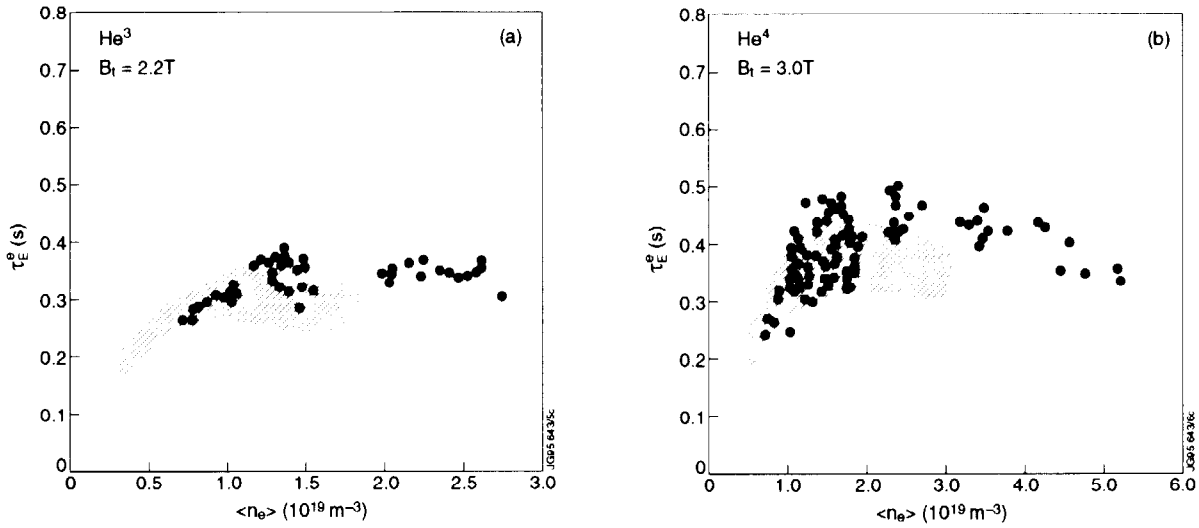

Figure 12. Electron energy replacement time versus volume averaged density for He plasmas a) He^3, I_p=2 MA, B_t=2.2 T, q_{cyl}=(2-3); b) He^4, I_p=3 MA, B_t=3 T, q_{cyl}=(3-4); in both cases the shaded areas correspond to the Deuterium results at the same plasma parameters.

VIII. SATURATED REGIME SCALINGS

The parametric scaling of confinement in the SOC regime has been investigated. If the Connor-Taylor constraints [14] are valid and no dependence on density is observed, the dependence of τ_E on size R and magnetic field B should be given by $B\ \tau_E = (R^5B^4)^a$ in the ohmic regime. A regression on the JET data in the SOC regime only, defined as $\langle n \rangle q_{cyl} > 5 \times 10^{19}$ m^{-3}, gives $\tau_E \propto B^{0.66\pm0.01}$. If the Deuterium concentration, given by the Z_{eff} value from visible bremsstrahlung assuming Carbon to be the main impurity, is used to estimate the ion energy content, the resulting scaling is only slightly different: $\tau_E \propto B^{0.61\pm0.01}$. A similar scaling has been found in TORE-SUPRA data [15]. However, both ASDEX and FTU have found a weaker

dependence [12,13]. In the case of FTU, $\tau_E \propto B^{0.3}$ is found at most, with a coupling between Z_{eff} and B_t dependences. In the case of JET, no clear coupling between B_t and Z_{eff} is observed. The size dependence corresponding to the JET scaling with B is $\tau_E \propto R^2$, which is not far from the usual size dependence in L mode plasmas. The FTU dependence would imply $\tau_E \propto R^{1.6}$.

Another scaling for the ohmic confinement has recently been proposed [15], which makes use of the Hugill number $H=5a^2\kappa\bar{n}\ /I_p$ as the relevant parameter for τ_E scaling with density. In figure 13, the JET Deuterium and Helium data are compared with this scaling. In the case of Helium the total energy content has been estimated using the assumption $T_i=T_e$ and the ion concentration from Z_{eff} measured by bremsstrahlung, assuming Carbon to be the main impurity. The scaling for τ_E in the SOC regime proposed by [15], $\tau_E^{sat} = 0.09\ a\ R\ B_t^{0.6}$ (s,m,T), and the scaling of the saturation density with $H\ B_t^{0.5}$ seems to be in agreement with the JET data.

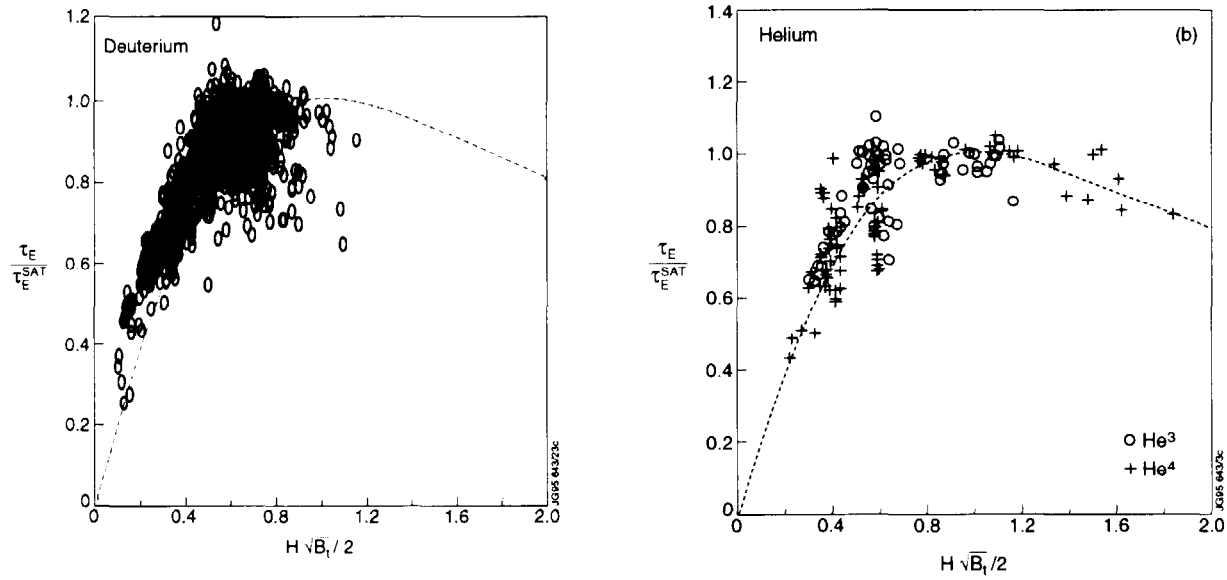

Figure 13. Global energy confinement time normalized to the TORE-SUPRA SOC scaling versus the Hugill number multiplied by $B_t^{1/2}/2$ for a) Deuterium plasmas; and b) for Helium plasmas; the dotted line is the scaling proposed by [15]

IX. CONCLUSIONS

A database of ohmic global energy confinement data has been assembled for JET with data from mainly Deuterium and Helium plasmas. The amount of Hydrogen data in this database is too small to assess differences in confinement between Hydrogen and Deuterium. Likewise the effects of plasma configuration and elongation on confinement cannot be distinguished. The trends of JET ohmic confinement, which can be assessed in the database, appear to be in qualitative agreement with the trends observed on other smaller tokamaks such as FTU and

ASDEX. The main difference is a stronger magnetic field dependence of τ_E which has also been observed on TORE SUPRA. The saturated ohmic confinement regime (SOC) is observed for $\langle n \rangle > 1.5 \times 10^{19}$ m^{-3} in JET when $q_{cyl} = 3.5$ and $B_t = 3T$. In the SOC regime, the stronger magnetic field dependence corresponds to a length scale of $\tau_E \propto R^2$, if the Connor-Taylor constraints are satisfied. Apart from that, no attempt has been made in this paper to estimate the dependence of the energy confinement on tokamak size in the ohmic regime. However, the data contained in this database, together with data from other tokamaks, would permit this problem to be addressed.

REFERENCES

[1] F. Wagner and U. Stroth, Plasma Phys. Control. Fusion 35 (1993) 1321.

[2] D. V. Bartlett, et al., Nuclear Fusion **28** (1988) 73.

[3] F. Tibone, et al., Nuclear Fusion **33** (1993) 1319.

[4] J.P. Christiansen, Report JET-R(86)**04** and Journal of Computational Physics **73** (1987) 85.

[5] R.E. Waltz, et al., Nuclear Fusion **26** (1986) 1729.

[6] F. Alladio, et al., Controlled Fusion and Plasma Physics, Proc. 19th European Conf. (Innsbruck,1992) Vol.1, 23.

[7] INTOR Group, International Tokamak Reactor, phase Two A, Part II,(Rep. Int. Workshop Vienna 1984 and 1985) IAEA, Vienna (1986) 494.

[8] K. Lackner and N.A.O. Gottardi, Nuclear Fusion **30**(1990) 767.

[9] P.N. Yushmanov, et al., Nuclear Fusion, **30**(1990) 1999.

[10] M. Greenwald, et al., Plasma physics and Controlled nuclear Fusion Research, Proc. 15th Int. Conf. 1994 (Seville) IAEA-CN-60/A2/4-P-2.

[11] G. Bracco, et al., Controlled Fusion and Plasma Physics, Proc. 21th European Conf. (Montpellier,1994) Vol.1, 70.

[12] P.J. McCarthy, et al., Nuclear Fusion **31**(1991)1595.

[13] F. Alladio, et al., Plasma physics and Controlled nuclear Fusion Research, Proc. 15th Int. Conf. 1994 (Seville) IAEA-CN-60/A2/4-P-3.

[14] J.W Connor and J.B. Taylor, Nuclear Fusion **17**(1977) 1047.

[15] X.L. Zou., et al., Controlled Fusion and Plasma Physics, Proc. 22th European Conf. (Bournemouth,1995).